Medicinal Chemistry Research (2019) 28:1272–1283
https://doi.org/10.1007/s00044-019-02372-y

MEDICINAL CHEMISTRY RESEARCH

ORIGINAL RESEARCH

New fluoroquinolones/nitric oxide donor hybrids: design, synthesis and antitubercular activity

Hossameldin A. Aziz[1] · Gamal A. I. Moustafa[1] · Samar H. Abbas[1] · Glenn Hauk[2] · Vagolu Siva Krishna[3] · Dharmarajan Sriram[3] · James M. Berger[2] · Gamal El-Din A. Abuo-Rahma[1]

Received: 8 January 2019 / Accepted: 22 May 2019 / Published online: 6 June 2019

Abstract

New nitric oxide (NO) donating fluoroquinolones/nitrate ester hybrids were prepared and their structures were characterized by various spectroscopic and analytical tools. The release of NO from the prepared nitrate esters was measured using the modified Griess colorimetric method. Evaluation of antitubercular activity showed that most of tested compounds exhibited comparable or higher activity than the parent fluoroquinolones. Compounds **2b**, **3a**, **4a**, **5a**, and **2d** showed better activity than ciprofloxacin. Nevertheless, none of the new compounds were superior to the parent fluoroquinolones in terms of DNA cleavage stimulation in mycobacteria. The additional growth inhibition effect that is distinct from gyrase poisoning may be due to release of NO or enhancement of lipophilicity. These data are augmented by docking results where the docked compounds did not exert additional significant bindings over the parent fluoroquinolones.

Keywords Fluoroquinolones · Antitubercular · Nitric oxide (NO) · Cleavable DNA complex · Molecular docking

Introduction

Tuberculosis (TB) is one of the most serious global health problems (World Health Organization 2017), It is caused by *M. tuberculosi.s* (Miltgen et al. 2002; Bryskier and Lowther 2002). In 2016, TB is considered the 9th leading cause of death worldwide and is the top cause from a single infectious agent, ranking above HIV/AIDS (Khaund et al. 2018). TB Treatment is generally difficult and requires administration of multiple antibiotics over a long period of time (AKoch et al. 2018). The emergence of multi-drug-resistant TB (MDR-TB) and the extensively drug-resistant TB (XDR-TB) has increased the difficulty for managing this serious disease (Sotgiu and Migliori 2015; Guerrini et al. 2013). As a result, there has been a growing interest for discovering new antitubercular drugs that can combat drug-resistant and drug-sensitive forms of TB.

Fluoroquinolones are synthetic bactericidal agents that act by interfering with two essential bacterial enzymes, DNA Gyrase and Topoisomerase IV, which are essential for transcription and DNA replication, respectively (Champoux 2001; Hooper 2001). It is known that DNA gyrase is the unique topoisomerase target for quinolones in *M. tuberculosis* (Aubry et al. 2004). Furthermore, the quinolone core is a critical component of compounds possessing promising antitubercular activity (Talath and Gadad 2006; Vaitilingam et al. 2004). Currently, clinical studies have shown that moxifloxacin, gatifloxacin and ciprofloxacin are valuable second-line agents in the treatment of TB (Gillespie et al. 2014; Merle et al. 2014). Research has indicated that the introduction of substituents on *N*-4 piperazinyl moiety of quinolones can improve physiochemical properties, reduce zwitter-ion character, and increase lipophilicity, one of the most important parameters in designing new antitubercular agents (Abdel-Aziz et al. 2013; Abuo-Rahma et al. 2009; Sriram et al. 2005).

Nitric oxide (NO) is a lipophilic gas that affects numerous critical functions in the body (Vahora et al. 2016;

✉ Samar H. Abbas
samar_hafez@mu.edu.eg

✉ Gamal El-Din A. Abuo-Rahma
gamal.aborahma@mu.edu.eg

[1] Department of Medicinal Chemistry, Faculty of Pharmacy, Minia University, Minia Minia-61519, Egypt

[2] Department of Biophysics and Biophysical Chemistry, Johns Hopkins University, School of Medicine, Baltimore, MD 21205, USA

[3] Department of Pharmacy, Birla Institute of Technology and Science, Pilani, Hyderabad Campus, Hyderabad, India

Trinity et al. 2015; Pitsikas 2015; Böhmer et al. 2015; Shi et al. 2000; Cooke et al. 2000). It was discovered by Furchgott, Ingnarro and Murad, for which they shared a Nobel Prize in 1998 (Fang 2004). Several reports have referred to the antibacterial activity of NO, resulting from its ability to diffuse through lipid bilayer membrane (Clementi et al. 1999) and directly act upon metalloproteins, thereby inhibiting respiratory activity, protein and DNA damage and apoptosis (Gardner et al. 1997; D'Autréaux et al. 2002; Porasuphatana et al. 2003; Timmins et al. 2004). Moreover, it was demonstrated that the frontline antitubercular drug, isoniazid (INH) can act through an INH-derived NO that is formed by the oxidative activation of INH by KatG (Bi et al. 2015). Hybrid NO donor drugs thus represents an important approach to the design of NO-donating compounds. This is a broad grouping that covers a range of established drugs that have been structurally modified to incorporate NO-containing molecules (Ciccone et al. 2003; Long et al. 1999). The aim of such strategies is to synthesize drugs that enhance the pharmacological activity of the parent compound (Chugunova et al. 2016) or lower their side effects (Wallace et al. 1994).

The present work aims to design a new NO-donating series of *N*-4-piperazinyl ciprofloxacin or norfloxacin/nitrate ester hybrids for the purpose of synergism and the improvement of physiochemical properties of fluoroquinolones by integrating two bioactive entities: the fluoroquinolone scaffold and the NO donor moiety. We measured the release of NO from the nitrate ester derivatives in vitro by modified Griess method (Aziz et al. 2017). DNA-Gyrase assay and docking studies also were carried out to determine the extent to which antitubercular activity is related to gyrase inhibition in vitro.

Result and discussion

Chemistry

Synthesis of the target compounds 3a–d and 5a–b

The target compounds were synthesized as outlined in Scheme 1. Acylated derivatives of ciprofloxacin and norfloxacin **2a–b** and **2c–d**, respectively, were synthesized by biphasic reaction (Mohammed et al. 2016; Ahmed et al. 2018) through acylation of ciprofloxacin or norfloxacin with bromoacetyl bromide or 3-bromopropionyl chloride in dichloromethane in presence of potassium carbonate. Intermediates **4a** and **4b** were prepared by addition of ciprofloxacin or norfloxacin, respectively, to a mixed anhydride formed in situ by treatment of 2-bromopropionic acid with ethyl chloroformate in the presence of TEA. Conversion of acyl bromide derivatives **2a–d** and **4a–b** into the respective NO-donating nitrate esters **3a–d** and **5a–b** was achieved by heating compounds **2a–d** and **4a–b** with silver nitrate in acetonitrile. The IR spectra show asymmetric stretching of

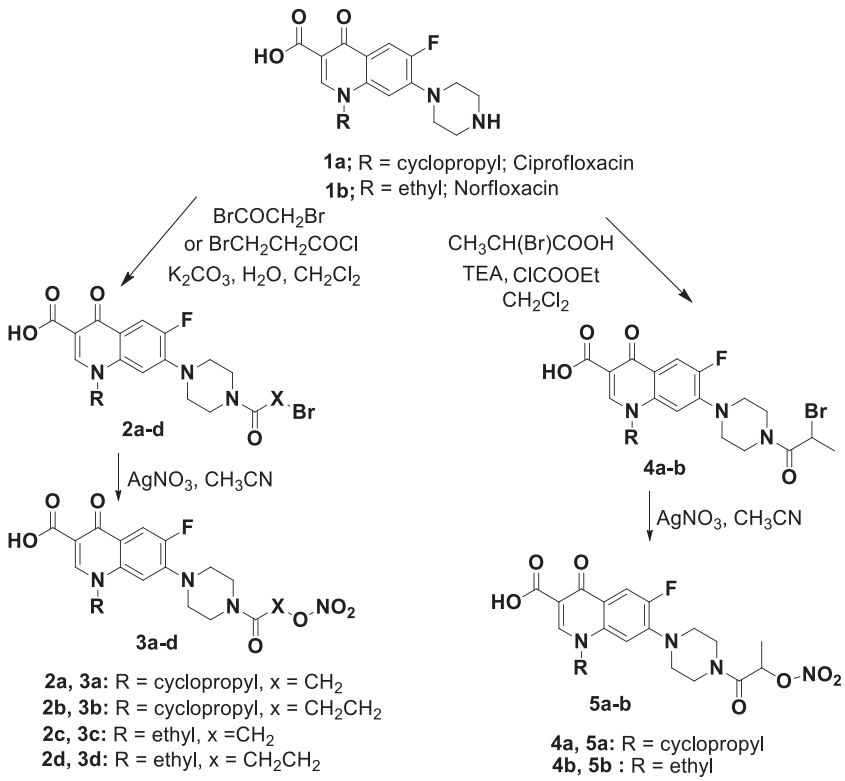

Scheme 1 Synthesis of the target compounds **3a–d** and **5a–b**

ONO_2 at 1500–1544 cm^{-1} and symmetric stretching at 1280–1294 cm^{-1}. ^1H NMR spectra of the prepared nitrate esters **3a–d** and **5a–b** show the typical characteristic pattern of ciprofloxacin and norfloxacin. Replacement of bromine atom in compounds **2** and **4** by **ONO_2** in compounds **3** and **5** led to a downfield shift of methylene protons by 1.10–1.26 ppm and by 0.79–0.82 ppm of the methine proton, respectively. ^{13}C NMR spectra of nitrate esters showed the typical characteristic pattern of ciprofloxacin and norfloxacin. It was found that replacement of bromide by nitrate caused downfield shift of the neighboring carbon by 40.90–41.04 ppm.

Measurement of NO release using a modified Griess method

The release of NO from the target NO-donating hybrids **3a–d** and **5a–b** was measured by a modified version of the Griess method (Aziz et al. 2017) in which 4-nitroaniline was used instead of sulfanilamide. NO release was measured at 100 µM concentration of the tested compounds and assessed in the stable nitrite form relative to that of a standard sodium nitrite solution and calculated as amount of NO released (mol/mol) %. As shown in Table 1, the release of NO from **5a** and **5b** was slightly lower than other nitrate derivatives and may originate from steric hindrance added by the α-methyl group.

Table 1 The amount of NO released from compounds **3a–d** and **5a–b** in phosphate buffer of pH = 7.4 ($n = 3$)

Compound Number	Amount of NO released % (mol/mol)
3a	5.29 ± 0.03
3b	4.72 ± 0.05
3c	5.01 ± 0.09
3d	4.83 ± 0.03
5a	4.13 ± 0.01
5b	4.27 ± 0.01

Biological evaluation

Evaluation of antimycobacterial activity

In vitro screening of the synthesized compounds against *M. tuberculosis* The in vitro antimycobacterial activity of synthesized compounds **2a–d**, **3a–d**, **4a–b**, and **5a–b** against *M. tuberculosis* H37Rv strain was evaluated. The cLogP values of synthesized compounds were calculated by ChemDraw Professional 15.1 to provide an estimate of their lipophilicity (Table 2). The calculation of correlation coefficient between cLogP and activity against *M. tuberculosis* indicates that the R value is −0.2861. This means the relationship between theoretical calculated cLogP and activity is only weak, this means that increase log$P$ will decrease activity slightly. This correlation could be not the same between the activity and actual lipophilicity in the cells because of it is very difficult to accurately assess the lipophilicity of molecules such as fluoroquinolones having zwitterion characters on the basis of theoretical methods that do not address all the thermodynamic phenomena occurring between the molecules and surrounding the environment (Kłosińska-Szmurło et al. 2014; Abou Rahma et al. 2018).

As shown in Table 2, bromoacyl derivatives **2b** and **4a** and nitrate ester derivatives **3a** and **5a** displayed slightly higher potency against *M. tuberculosis* H37Rv (MIC range: 1.7–1.8 µM) than ciprofloxacin (MIC = 2.4 µM). Moreover, norfloxacin derivatives **2d** and **4b** are more potent against *M. tuberculosis* H37Rv (MICs range: 1.4–3.4 µM) than norfloxacin (MIC = 9.8 µM), whereas compounds **2c**, **3c**, **3d**, and **5b** displayed comparable activity to norfloxacin. It is noteworthy that norfloxacin derivative **2d** showed higher activity than both ciprofloxacin and norfloxacin.

In general, the prepared ciprofloxacin derivatives are more potent than their corresponding norfloxacin derivatives. Notably, introduction of a *N*-4 piperazinyl substitution in the norfloxacin skeleton improved antitubercular

Table 2 The MICs of the tested compounds against *M. tuberculosis* (µM) and their cLog$P$ values

Compound	MIC against *M. tuberculosis* (µM)	cLogP	Compound	MIC against *M. tuberculosis* (µM)	cLog$P$
2a	**3.4**	1.893	**2c**	7.1	1.838
2b	**1.7**	1.872	**2d**	**1.4**	1.817
3a	**1.8**	−0.409	**3c**	7.4	−0.464
3b	**3.5**	−0.303	**3d**	7.2	−0.385
4a	**1.7**	2.422	**4b**	**3.4**	2.367
5a	**1.7**	−0.099	**5b**	7.2	−0.155
Ciprofloxacin	**2.4**	−0.725	**Norfloxacin**	9.8	−0.780

The bold value indicated the most active compounds

activity compared to analogous modifications of the ciprofloxacin skeleton. We observed that norfloxacin bromoacyl derivatives **2c**, **2d**, and **4b** exhibited higher potency than norfloxacin itself. This result may be explained by an increased ability to penetrate the hydrophobic mycobacterial cell wall due to the greater lipophilicity, as reflected in cLog*P* values (Table 2). In particular, compound **2d** exhibited a sevenfold increase in activity over norfloxacin. Converting bromoacyl derivatives **2c**, **2d**, and **4b** into their corresponding nitrate esters **3c**, **3d**, and **5b** reduced their antimycobacterial activity. Nevertheless, those nitrate esters proved slightly more potent than norfloxacin, which may be explained by a slightly higher lipophilicity than norfloxacin, and/or by NO release from those compounds. Considering the synthesized ciprofloxacin analogues, the bromoacyl derivatives **2b** and **4a** and nitrate ester derivatives of ciprofloxacin **3a** and **5a** are generally more potent than ciprofloxacin. The higher antimycobacterial activity of **2b** and **4a** may derive from the increased lipophilicity of the *N*-4-Piperazinyl substitution. The slightly higher antimycobacterial activity of nitrate ester **3a**, compared to bromoacyl analogue **2a** may be explained by its ability to release NO. Overall, the results obtained in this study strengthen the argument that the lipophilicity of the fluoroquinolone scaffold and its penetration into mycobacteria is not the sole factor controlling antitubercular activity. *N*-4-Piperazinyl substitutions may hamper the interaction of the molecule with essential residues in the target proteins within mycobacteria.

DNA cleavage assay

DNA gyrase is a heterotetrameric ($GyrA_2GyrB_2$) enzyme that transiently forms double-stranded DNA breaks as it negatively supercoils DNA (Aldred et al., 2014). Fluoroquinolones prevent break resealing following DNA strand passage; leading to persistent covalent enzyme–DNA adducts called cleaved complexes. Cleaved-complex formation in turn inhibits bacterial growth (Barrett et al. 1993).

The formation of gyrase-dependent, cleaved-DNA complexes upon fluoroquinolone treatment can be readily monitored by native agarose gel electrophoresis. The ability of our synthesized compounds to generate cleaved complexes was assessed by measuring the formation of linear DNA from a starting supercoiled plasmid, using ciprofloxacin as a reference. The inhibition of DNA supercoil relaxation and the promotion of DNA cleavage were monitored by running gels in the absence or presence of ethidium bromide (a DNA intercalating agent), respectively; the addition of ethidium bromide leads to positive supercoiling of closed-circular DNA species, allowing us to readily resolve relaxed DNA from nicked and linear species. For this study, compounds **2d**, **3a**, **3b**, **4a**, and **5b** were selected to investigate their ability to promote DNA cleavage by *M. tuberculosis* gyrase. Of the tested bromoacyl derivatives, only compound **4a** induced DNA cleavage (at ~125 µM concentration). By comparison, compound **2d** did not produce a clear cleavage signal (Fig. 1).

As for the tested nitrate esters, compound **3a** poisoned DNA gyrase by inducing DNA cleavage by 25 µM, whereas

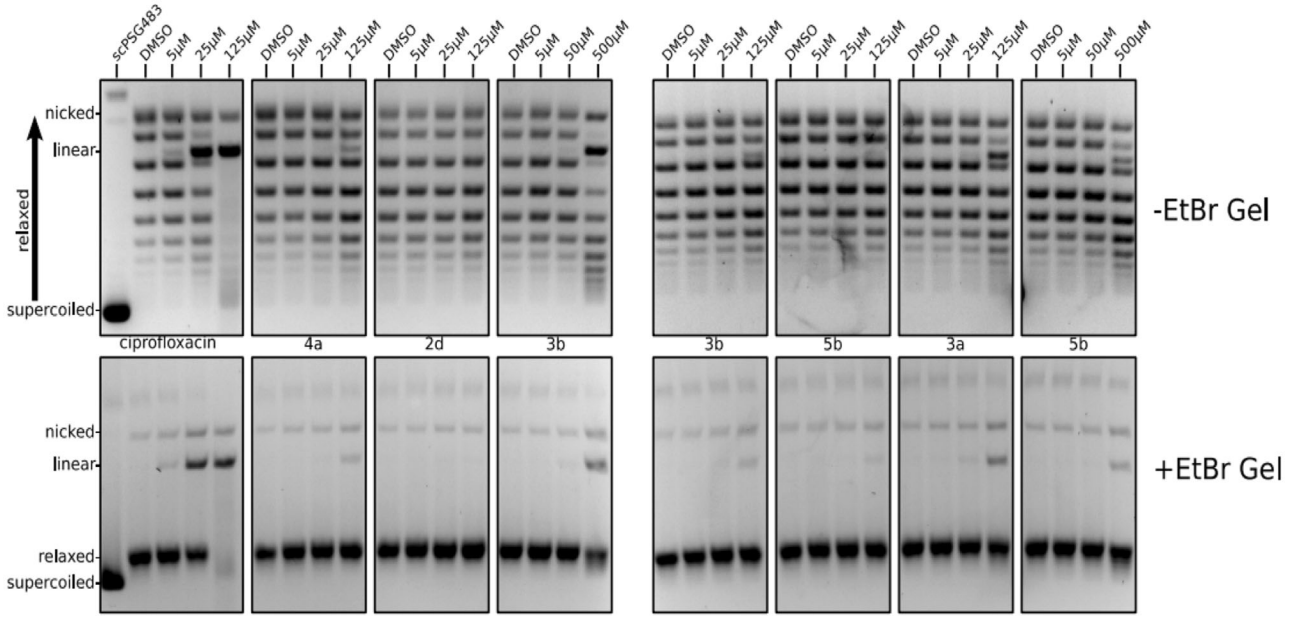

Fig. 1 DNA cleavage by MTB gyrase induced by ciprofloxacin, **2d**, **3a**, **3b**, **4a**, and **5b**

Table 3 ΔG values (kcal/mol) of the tested compounds, ciprofloxacin, and moxifloxacin

Compound	ΔG values (kcal/mol)	Compound	ΔG values (kcal/mol)
Moxifloxacin	–11.28	**3c**	–8.93
Ciprofloxacin	–7.88	**3d**	–10.92
2b	–8.88	**4a**	–9.43
2c	–9.63	**4b**	–11.37
2d	–9.47	**5a**	–15.01
3a	–13.90	**5b**	–10.97
3b	–10.66		

The bold value indicated the most active compounds

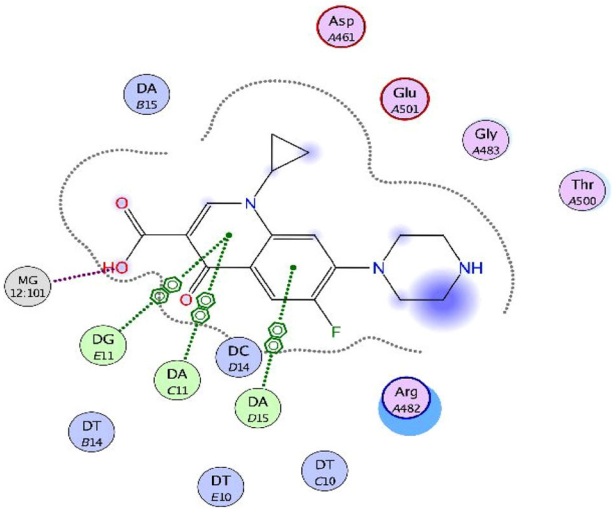

Fig. 2 2D Diagram of **ciprofloxacin** docked into the active site of MTB DNA gyrase

3b produced cleavage products at higher concentration (50–125 μM). Nitrate ester **5b** only induced DNA cleavage at the highest concentration tested (500 μM) (Fig. 1). A general overview of the experimental data obtained for the tested compounds revealed that the new compounds have improved MICs compared to the parent fluoroquinolones (within threefold of each other), but very different impacts on DNA cleavage, and that none of the new compounds were superior to the parent fluoroquinolones in terms of cleavage stimulation. Thus, the new compounds are exerting an additional growth inhibition effect that is distinct from gyrase poisoning.

In vitro cytotoxicity screening

Compounds **2a**, **2b**, **2d**, **3a**, **3b**, **3c**, **3d**, **4a**, and **4b** were tested at a single concentration of 10 μM against 60 cancer cell lines in National Cancer Institute (NCI). In general, most of the tested compounds showed no cytotoxic activity against tested cell lines (results in details in supplementary data (http://www.dtp.nci.nih.gov)).

Docking studies

To gain insights into how the fluoroquinolone derivatives might associate with Gyrase, we carried out docking simulations using Molecular Operating Environment (MOE®) version 2014.09, Chemical Computing Group Inc., Montreal, Canada. The docking study was carried out for all synthesized compounds based on the crystal structure of moxifloxacin- and DNA-bound MTB gyrase (PDB: 5bs8) (Blower et al. 2016). All of the tested compounds appear to have affinity for the enzyme, with binding free energy (ΔG) values ranging from −8.88 to −15.01 kcal/mol. These values are comparable to the reference compounds, moxifloxacin ($\Delta G = -$**11.28** kcal/mol) and ciprofloxacin ($\Delta G =$ −**7.88** kcal/mol) (Table 3). The correlations between docking scores of the synthesized compound and the activity against *M. tuberculosis* or the theoretical calculated cLog*P* indicate that the relationship between docking score and these two variables are only weak.

The most potent nitrate ester compound **3a** which poisoned gyrase enzyme at 25–125 μM showed the best binding score among the docked compounds tested for gyrase enzyme activity.

Concerning the docking study of the synthesized compounds, the binding-score energies have negative values, suggesting that the binding of quinolone derivatives to the active site of Gyrase enzyme may be rapid. The docking study also showed that the target compounds ligand a magnesium ion in a manner similar to the reference moxifloxacin or ciprofloxacin (Fig. 2, Fig. 3), through the *C*-3 carboxylic group and *C*-4 carbonyl functionality, hydrophobic interaction with the active site of the gyrase enzyme, hydrogen bonding with amino acid residue Arg128 and van der Walls interaction with nucleotide bases through quinolone moiety or the introduced *N*-4 piperazinyl moiety. Furthermore, nitrate ester **3a** promotes extra van der Waals and hydrogen bonding interaction with gyrase amino acids (e.g., Arg. B482) (Fig. 4, Fig. 5).

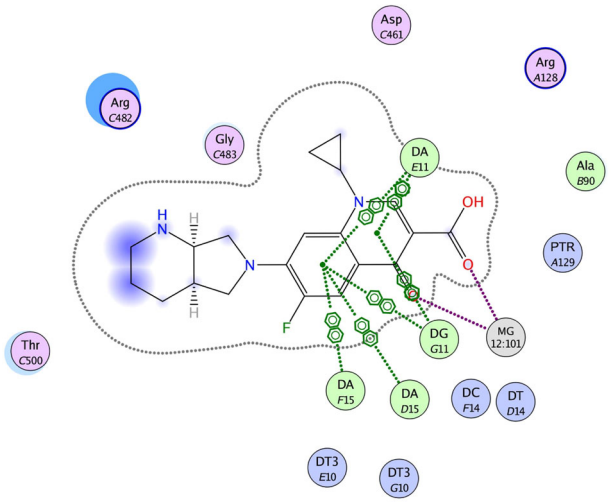

Fig. 3 2D Diagram of **moxifloxacin** docked into the active site of MTB DNA gyrase

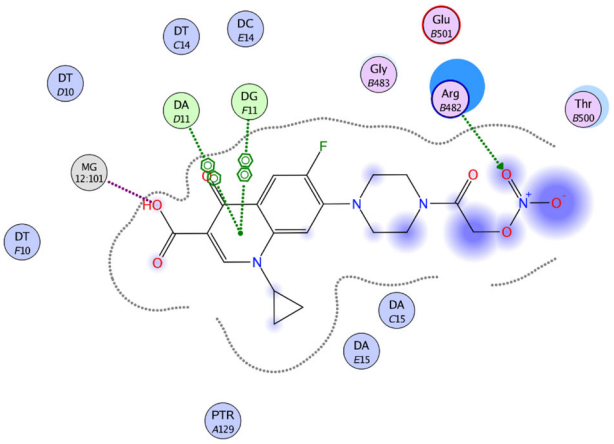

Fig. 4 2D Diagram of compound **3a** docked into the active site of MTB DNA gyrase

The most active norfloxacin derivative **2d** showed additional van der Waal interactions with surrounding nucleotide bases of DNA (Fig. 6, Fig. 7). Nevertheless, in general, all the docked compounds did not exert additional significant bindings over the parent fluoroquinolones; ciprofloxacin or norfloxacin, which is also supported by the in vitro DNA cleavable complex formation shown in Fig. 1.

Conclusion

New fluoroquinolone/NO donor hybrids were synthesized, characterized by various spectroscopic tools and evaluated for their in vitro antitubercular activity against *M. tuberculosis* H37Rv. Introduction of *N*-4 piperazinyl substitution in norfloxacin skeleton improved antitubercular activity greatly. Results revealed that the bromoacyl derivatives **2b**, **2d**, **4a**, and **4b** and nitrate ester derivatives **3a** and **5a** showed higher activity against *M. tuberculosis* H37Rv (MICs 1.4–1.8 μM) than their parent quinolones. The lack of a relationship between the MICs and cLog*P* values of the synthesized compounds strengthens the argument that the lipophilicity is not the only factor that affects the antimycobacterial activity. Despite the comparative or higher antimycobacterial activity of some of the newly synthesized compounds to ciprofloxacin, they produced lower levels of cleaved DNA than ciprofloxacin indicating the intermediacy of another mechanism besides DNA gyrase inhibition, such as the possible release of NO or enhancement of lipophilicity.

Experimental section

Chemistry

The reactions were monitored by TLC using Methylene chloride: Methanol (9.5: 0.5 V/V). Melting points were determined on an electrothermal melting point apparatus (Stuart Scientific Co.) and were uncorrected. IR spectra are recorded as KBr disks on a Shimaduz 408 instrument Spectrophotometer at the Faculty of Science, Sohag University. NMR Spectra were taken on a Bruker AM NMR (400 MHz) spectrometer at Faculty of Science, Sohag University. All numbers referring to NMR data obtained are in parts per million (ppm). Elemental microanalyses for carbon, hydrogen, and nitrogen were performed at The Regional Center for Mycology and Biotechnology, Al-Azhar University, Cairo, Egypt. For TLC, the DC Alufolien, Kieselgel 60 F254 precoated plates are used (Merck, Darmastadt, Germany). HRMS spectra were collected *via*-Thermo Scientific Q Exactive™ Orbitrap mass spectrometer and reported as mass/charge (*m/z*) with percent relative abundance, Faculty of Pharmaceutical Sciences, University of British Columbia, Vancouver Campus, Canada.

General procedure of synthesis of acylated fluoroquinolones 2a–d

To a stirred solution of ciprofloxacin or norfloxacin (1 mmol) in DCM (30 mL) a solution of potassium carbonate (1.1 mmol) in distilled water (30 mL) was added at 0–5 °C. Bromoacetyl bromide (or 3-bromopropionyl chloride) (5.5° mmol) in DCM (15 mL) was slowly added over a period of 30 min. Stirring was continued for 2 h at 0–5 °C, then at room temperature for additional 12 h. The whole mixture was then transferred to a separating funnel where it was extracted with DCM and washed successively with 1 *N* HCl (2 × 25 mL) and water (2 × 25 mL). The organic layer was separated, dried over anhydrous sodium

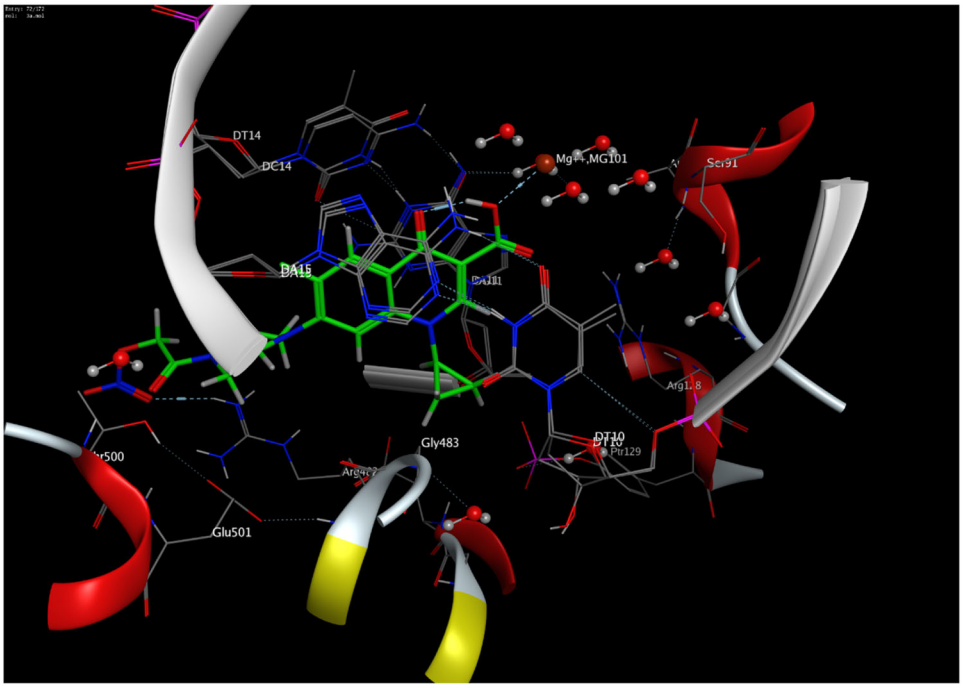

Fig. 5 3D Diagram of compound **3a** docked into the active site of MTB DNA gyrase

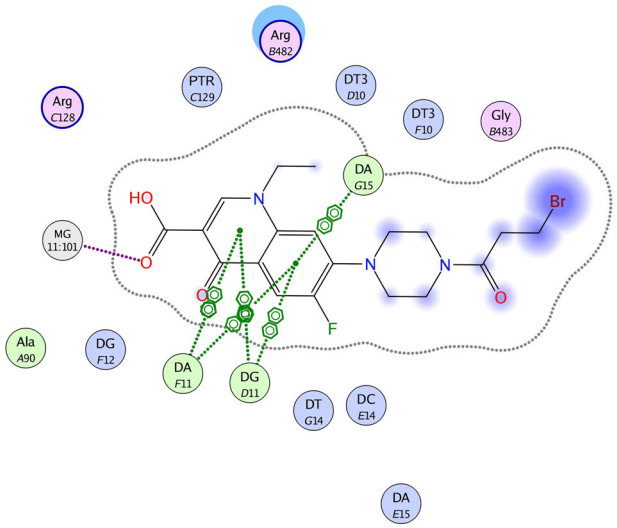

Fig. 6 2D Diagram of compound **2d** docked into the active site of MTB DNA gyrase

sulfate, filtered off and evaporated under reduced pressure to give acylated derivatives **2a–d**.

7-(4-(2-Bromoacetyl) piperazin-1-yl)-1-cyclopropyl-6-fluoro-1,4-dihydro-4-oxoquinoline-3-carboxylic acid 2a Yellow powder; yield: 0.413 g (95%); mp: 263 °C, IR (KBr) ύ (cm^{-1}): 3271 (NH), 1726 (carboxylic C = O), 1651 (amidic C = O) and 1621 (4-keto C = O); ^{1}H-NMR (400 MHz, DMSO-d_6) δ ppm: 1.21–1.25 (2 H, m, cyclopropyl-2H), 1.31–1.37 (2 H, m, cyclopropyl-2H), 3.37–3.47 (4 H, m, piperazinyl-H), 3.62–3.75 (4 H, m, piperazinyl-H), 3.82–3.88 (1 H, m, cyclopropyl-H), 4.22 (2 H, s, CH_2Br), 7.60 (1 H, d, $J_{H\text{-}F}$ = 6.8 Hz, H8), 7.94 (1 H, d, $J_{H\text{-}F}$ = 13.6 Hz, H5), 8.68 (1 H, s, H2), 15.11 (1 H, s, COOH). Anal. Calcd for $C_{19}H_{19}BrFN_3O_4$: C, 50.46; H, 4.23; N, 9.29. Found: C, 50.78; H, 4.34; N, 9.47 (Mustaev et al. 2014).

7-(4-(3-Bromopropanoyl)piperazin-1-yl)-1-cyclopropyl-6-fluoro-1,4-dihydro-4-oxoquinoline-3-carboxylic acid 2b Yellow powder; yield: 0.400 g (85%); mp: 247 °C; IR (KBr) ύ (cm^{-1}): 3271 (NH), 1726 (carboxylic C = O), 1651 (amidic C = O) and 1621 (4-keto C = O); ^{1}H-NMR (400 MHz, DMSO-d_6)δ ppm: 1.23–1.28 (2 H, m, cyclopropyl-H), 1.41–1.46 (2 H, m, cyclopropyl-H), 3.02 (2 H, t, J = 6.8 Hz, $BrCH_2C\underline{H}_2$), 3.32–3.42 (4 H, m, piperazinyl-H), 3.54–3.62 (1 H, m, cyclopropyl-H), 3.72 (2 H, t, J = 6.8 Hz, $BrC\underline{H}_2CH_2$), 3.74-3.80 (2 H, m, piperazinyl-H), 3.91–3.97 (2 H, m, piperazinyl-H), 7.44 (1 H, d, $J_{H\text{-}F}$ = 6.8 Hz, H8), 8.06 (1 H, d, $J_{H\text{-}F}$ = 12.8 Hz, H5), 8.78 (1 H, s, H2), 14.92 (1 H, s, COOH); ^{13}C-NMR (100 MHz, DMSO-d_6): 8.06, 29.36, 35.82, 36.37, 41.29, 44.87, 49.62, 50.09, 106.98, 111.50 (d, J = 23 Hz), 119.28, 119.36, 139.62, 145.35, (d, J = 10 Hz), 148.59, 154.66, 166.39, 168.05, 176.80; Anal. Calcd for $C_{20}H_{21}BrFN_3O_4$: C, 51.51; H, 4.54; N, 9.01. Found: C, 51.79; H, 4.60; N, 9.13.

7-(4-(2-Bromoacetyl) piperazin-1-yl)-1-ethyl-6-fluoro-1,4 dihydro-4-oxoquinoline-3-carboxylic acid 2c White powder; yield: 0.370 g (84%); mp: 247–249 °C as reported (Aziz et al. 2017).

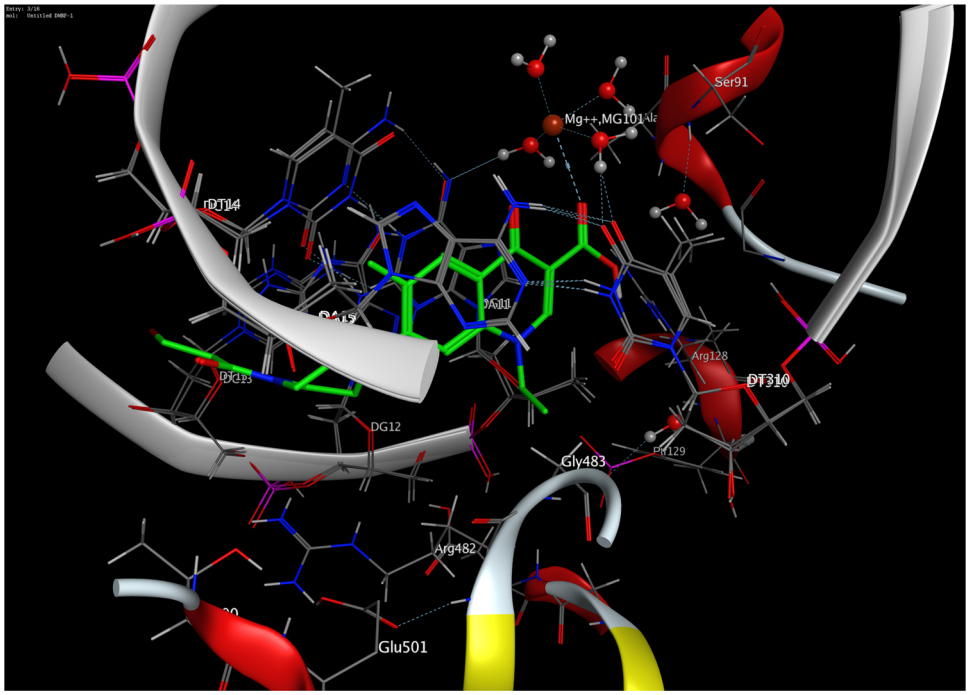

Fig. 7 3D Diagram of compound **2d** docked into the active site of MTB DNA gyrase

7-(4-(3-Bromopropanoyl)piperazin-1-yl)-1-ethyl-6-fluoro-1,4-dihydro-4-oxoquinoline-3-carboxylic acid 2d Pale yellow powder; yield: 0.398 g (88%); mp: 247–248 °C; ^{1}H-NMR (400 MHz, DMSO-d_6)δ ppm: 1.44 (3 H, t, J = 7.2 Hz, N $CH_2\underline{CH_3}$), 3.04 (2 H, t, J = 6.8 Hz, $BrCH_2\underline{CH_2}CO$), 3.32–3.40 (4 H, m, piperazinyl-H), 3.66–3.74 (4 H, m, piperazinyl-H), 3.69 (2 H, t, J = 6.8 Hz, $BrCH_2\underline{CH_2}CO$), 4.59 (2 H, q, J = 7.2 Hz, N $CH_2\underline{CH_3}$), 7.20 (1 H, d, J = 7.2 Hz, H8), 7.93 (1 H, d, J = 14.2 Hz, H5), 8.93 (1 H, s, H2), 15.24 (1 H, s, COOH).^{13}C-NMR (100 MHz, DMSO-d_6): 14.79, 29.20, 35.90, 44.99, 49.53, 49.73 50.15, 106.56, 107.71, 111.74 (d, J = 23 Hz), 120.04, 137.69, 145.61 (d, J = 10 Hz), 148.96, 153.29 (d, J = 247 Hz), 166.45, 168.68 and 176.67; Anal. Calcd for $C_{19}H_{21}BrFN_3O_4$: C, 50.23; H, 4.66; N, 9.25. Found: C, 50.49; H, 4.72; N, 9.42.

General procedure of synthesis of new nitrate esters 3a–d

To a stirred solution of bromoacyl derivatives **2a–d** or **4a–b** (1 mmol) in acetonitrile (20 mL), sliver nitrate (4 mmol) in acetonitrile (20 mL) was added portion wise and the mixture was heated for 12–16 h at 80 °C. The formed precipitate of silver bromide was filtered, and the filtrate was evaporated till dryness, dissolved in DCM (30 mL) and washed with distilled water (2 × 25 mL) and brine (2 × 25 mL). The organic layer was dried over anhydrous sodium sulfate, filtered off and evaporated under reduced pressure. The residue was crystallized from the appropriate solvent to give nitrate esters **3a–d or 5a–b**.

1-Cyclopropyl-6-flouro-7-(4-(2-(nitrooxy)acetyl)piperazin-1-yl)-4-oxo-1,4-dihydroquinoline-3-carboxylic acid 3a Yellow crystals (methanol); yield: 0.203 g (47%); mp: 220–221 °C; IR (KBr) ύ (cm^{-1}): 3062 (NH), 1727 (carboxylic C = O) 1672, (amidic) and 1626 (4-keto C = O), 1500 and 1238 (ONO_2); ^{1}H-NMR (400 MHz, DMSO-d_6)δ ppm: 1.20–1.25 (2 H, m, cyclopropyl-H), 1.31–1.38 (2 H, m, cyclopropyl-H), 3.40–3.50 (4 H, m, piperazinyl-H), 3.62–3.75 (4 H, m, piperazinyl-H), 3.82–3.90 (1 H, m, cyclopropyl-H), 5.46 (2 H, s, CH_2ONO_2), 7.59 (1 H, d, $J_{H\text{-}F}$ = 6.8 Hz, H8), 7.94 (1 H, d, $J_{H\text{-}F}$ = 13.6 Hz, H5), 8.68 (1 H, s, H2), 15.07 (1 H, s, COOH); ^{13}C-NMR (100 MHz, DMSO-d_6): 8.06, 36.32, 43.97, 49.58, 69.33, 107.13, 107.45, 111.57 (d, J = 22 Hz), 119.50, 139.66, 145.16, 148.49, 153.42 (d, J = 247 Hz), 164.00, 166.25, 176.89; HRMS (ESI) calcd for $C_{19}H_{18}FN_4O$ $[M\text{-}H]^-$:433.1165, found: 433.1167.

1-Cyclopropyl-6-flouro-7-(4-(3-(nitrooxy)propanoyl)piperazin-1-yl)-4-oxo-1,4-dihydroquinoline-3-carboxylic acid 3b Yellow crystals (methanol); yield: 0.230 g (50%); mp: 217 °C; ^{1}H NMR (400 MHz, DMSO-d_6) δ ppm: 1.18-1.22 (2 H, m, cyclopropyl-H), 1.32–1.36 (2 H, m, cyclopropyl-H), 2.92 (2 H, t, J = 6.0 Hz, $CH_2\underline{CH_2}CO$), 3.35–3.45 (4 H, m, piperazinyl-H), 3.65–3.72 (4 H, m, piperazinyl-H),

3.79–3.87 (1 H, m, cyclopropyl-H), 4.82 (2 H, t, $J = 6.0$ Hz, $CH_2C\underline{H}_2ONO_2$), 7.58 (1 H, d, $J_{H\text{-}F} = 6.8$ Hz, H8), 7.94 (1 H, d, $J_{H\text{-}F} = 13.6$ Hz, H5), 8.68 (1 H, s, H2), 15.08 (1 H, s, COOH); ^{13}C NMR (100 MHz, DMSO-*d*$_6$): 8.05, 30.26, 36.30, 44.89, 49.56, 49.93, 70.26, 106.98, 107.43, 111.54 (d, $J = 22$ Hz), 119.32, 139.67, 145.24, 148.46, 152.16, 166.26, 167.85, 176.87; HRMS (ESI) calcd for $C_{20}H_{20}FN_4O_7$ $[M\text{-}H]^-$: 447.13212, found: 447.1325.

1-Ethyl-6-flouro-7-(4-(2-(nitrooxy)acetyl) piperazin-1-yl)-4-oxo-1,4-dihydroquinoline-3-carboxylic acid 3c Yellow crystals (acetonitrile); yield: 0.177 g (41.9%); mp: 201 °C as reported (Aziz et al. 2017).

1-Ethyl-6-flouro-7-(4-(3-(nitrooxy)propanoyl)piperazin-1-yl)-4-oxo-1,4-dihydroquinoline-3-carboxylic acid 3d Yellow crystals (acetonitrile); yield: 0.205 g (47%); mp: 199 °C; IR (KBr) ὁ (cm^{-1}): 1719 (carboxylic C = O), 1668 (amidic C = O), 1618 (4-keto C = O); ^{1}H NMR (400 MHz, DMSO-*d*$_6$)δ ppm: 1.44 (3 H, t, $J = 7.2$ Hz, $CH_2C\underline{H}_3$), 2.91 (2 H, t, $J = 6.0$ Hz, $CH_2C\underline{H}_2CO$), 3.33–3.42 (4 H, m, piperazinyl-H), 3.65–3.75 (4 H, m, piperazinyl-H), 4.58 (2 H, q, $J = 7.2$ Hz,$C\underline{H}_2CH_3$), 4.80 (2 H, t, $J = 6.0$ Hz, $CH_2C\underline{H}_2ONO_2$), 7.20 (1 H, d, $J_{H\text{-}F} = 7.6$ Hz, H8), 7.94 (1 H, d, $J = 13.6$ Hz, H5), 8.93 (1 H, s, H2), 15.23 (1 H, s, COOH); ^{13}C NMR (100 MHz, DMSO-*d*$_6$): 14.76, 30.26, 44.94, 49.53, 50.02, 70.26, 106.51, 107.74, 111.76 (d, $J = 23$ Hz), 120.04, 137.71, 145.59 (d, $J = 10$ Hz), 148.93, 153.28 (d, $J = 248$ Hz), 166.45, 167.85, 176.69; LC-MS (ESI) calcd for $C_{19}H_{21}FN_4NaO_7$ $[M + H]^+$: 437.15, found: 437.00

General procedure of synthesis of new acylated fluoroquinolones 4a and 4b

To a stirred solution of 2-bromopropionic acid (0.136 g, 1 mmol) in DCM (20 mL) triethylamine (0.131 g, 1.3 mmol) was added. The mixture was cooled in an ice bath (0–5 °C) and ethyl chloroformate (0.140 g, 1.3 mmol) was added portion wise. After being stirred for additional 40 min at the same temperature, ciprofloxacin or norfloxacin (1 mmol) was added and stirring was continued at room temperature for additional 12 h. The mixture was transferred to a separating funnel where it was washed successively with 1 N HCl (2 × 25 mL) and water (2 × 25 mL). The organic layer was separated, dried over anhydrous sodium sulfate, filtered off, and evaporated under reduced pressure to give acylated derivatives **2e** and **2f**, respectively.

7-(4-(2-Bromopropanoyl)piperazin-1-yl)-1-cyclopropyl-6-fluoro-1,4-dihydro-4-oxoquinoline-3-carboxylic acid 4a Yellow powder; yield: 0.335 g (72%); mp: 220 °C; ^{1}H NMR (400 MHz, DMSO-*d*$_6$) 1.18–1.25 (2 H, m, cyclopropyl-H), 1.31–1.37, (2 H, m, cyclopropyl-H), 1.57 (1.3 H, d, $J = 7.2$ Hz, $C\underline{H}_3CH$)*, 1.74 (1.7 H, d, $J = 7.2$ Hz, $C\underline{H}_3CH$)**, 3.35–3.45 (4 H, m, piperazinyl-H), 3.60–3.64 (1 H, m, cyclopropyl-H), 3.75–3.85 (4 H, m, piperazinyl-H), 5.12 (1 H, q, $J = 7.2$ Hz, $CH_3C\underline{H}$), 7.60 (1 H, d, $J_{H\text{-}F} = 6.8$ Hz, H8), 7.94 (1 H, d, $J_{H\text{-}F} = 13.6$ Hz, H5), 8.68 (1 H, s, H2), 14.93 (1 H, s, COOH).^{13}C NMR (100 MHz, DMSO-*d6*): 8.04, 15.05, 21.78, 36.39, 45.40, 49.69, 61.43, 107.23, 111.51 (d, $J = 22$ Hz), 119.38 (d, $J = 8$ Hz), 139.60, 145.19, 148.59, 153.42 (d, $J = 248$ Hz), 155.02, 166.38, 167.48 and 176.84; Anal. Calcd for $C_{20}H_{21}BrFN_3O_4$: C, 51.51; H, 4.54; N, 9.01. Found: C, 51.74; H, 4.65; N, 9.24.

N.B: the asterisk (*) refers to the signal of the minor rotamer, while the double asterisk (**) refers to the signal of the major rotamer.

7-(4-(2-Bromopropanoyl)piperazin-1-yl)-1-ethyl-6-fluoro-1,4-dihydro-4-oxoquinoline-3-carboxylic acid 4b Yellow powder; yield: 0.435 g (93%); mp: 228–230 °C; ^{1}H NMR (400 MHz, DMSO-*d*$_6$)δ ppm: 1.45 (3 H, t, 7.6 Hz, $NCH_2C\underline{H}_3$), 1.55 (1.1 H, d, $J = 7.2$ Hz, $C\underline{H}_3CH$)*, 1.71 (1.9 H, d, $J = 7.2$ HZ, $C\underline{H}_3CH$)**, 3.33–3.45 (4 H, m, piperazinyl-H), 3.60–3.82 (4 H, m, piperazinyl-H), 4.60 (2 H, q, $J = 7.2$ Hz, $N\ C\underline{H}_2CH_3$), 5.16 (1 H, q, $J = 7.2$ Hz, $CH_3C\underline{H}$), 7.21 (1 H, d, $J_{H\text{-}F} = 6.8$ Hz, H8), 7.94 (1 H, d, $J_{H\text{-}F} = 13.6$ Hz, H5), 8.97 (1 H, s, H2), 15.21 (1 H, s, COOH); ^{13}C NMR (100 MHz, DMSO-*d*$_6$): 14.87, 21.79, 41.92, 45.60, 49.55, 61.42, 106.79, 107.57, 111.71 (d, $J = 23$ Hz), 120.02 (d, $J = 8$ Hz), 137.60, 145.54 (d, $J = 10$ Hz), 149.10, 153.29 (d, $J = 248$ Hz), 166.56, 167.77, 176.65; Anal. Calcd for $C_{19}H_{21}BrFN_3O_4$: C, 50.23; H, 4.66; N, 9.25. Found: C, 50.38; H, 4.75; N, 9.38.

N.B: the asterisk (*) refers to the signal of the minor rotamer, while the double asterisk (**) refers to the signal of the major rotamer.

General procedure of synthesis of new nitrate esters 5a and 5b (as synthesis of 3a–d)

1-Cyclopropyl-6-flouro-7-(4-(2-nitrooxy)propanoyl)piperazin-1-yl)-4-oxo-1,4-dihydroquinoline-3-carboxylic acid 5a Yellow crystals (acetonitrile); yield: 0.190 g (42.6%); mp: 198 °C; ^{1}H NMR (400 MHz DMSO-*d*$_6$): 1.18–1.23 (2 H, m, cyclopropyl-H), 1.30–1.35 (2 H, m, cyclopropyl-H), 1.46 and 1.58 (3 H, d, $J = 7.2$ Hz, $CH\underline{CH}_3$), 3.30–3.35 (4 H, m, piperazinyl-H), 3.60–3.65 (1 H, m, cyclopropyl-H), 3.82–3.84 (4 H, m, piperazinyl-H), 5.94 (1 H, q, $\underline{CH}CH_3$), 7.61 (1 H, d, $J_{H\text{-}F} = 8$ Hz, H8), 7.95 (1 H, d, $J_{H\text{-}F} = 13.6$ Hz, H5), 8.69 (1 H, s, H2), 15.10 (1 H, s, COOH); ^{13}C NMR (100 MHz, DMSO-*d*$_6$): 8.04, 14.82, 36.30, 43.55, 49.69, 75.26, 107.27, 107.43, 111.56 (d, $J = 23$ Hz), 119.32, 139.67, 145.24, 148.46, 152.16, 166.26, 167.85, 176.87;

HRMS (ESI) calcd for $C_{20}H_{20}FN_4O_7[M\text{-}H]^-$: 447.1322, found: 447.1326.

1-Ethyl-6-flouro-7-(4-(2-nitrooxy)propanoyl)piperazin-1-yl)-4-oxo-1,4-dihydroquinoline-3-carboxylic acid 5b Yellow crystals (acetonitrile); yield: 0.39 g (88%); mp 190 °C; ^{1}H NMR (400 MHz, DMSO-d_6) δ ppm: 1.45 (3 H, t, $J = 7.2$ Hz, $CH_2\underline{CH_3}$), 1.46 (3 H, d, $J = 7.0$ Hz, $\underline{CH_3}CH$), 3.33–3.43 (4 H, m, piperazinyl-H), 3.75–3.85 (4 H, m, piperazinyl-H), 4.60 (2 H, q, $J = 7.2$ Hz, $\underline{CH_2}CH_3$), 5.95 (1 H, q, $J = 7.0$ Hz, $\underline{CH}CH_3$), 7.24 (1 H, d, $J_{H\text{-}F} = 7.6$ Hz, H8), 7.96 (1 H, d, $J_{H\text{-}F} = 13.6$ Hz, H5), 8.94 (1 H, s, H2), 15.21 (1 H, s, COOH); ^{13}C NMR (100 MHz, DMSO-d_6): 14.80, 44.881, 48.50, 49.80, 60.10, 75.96, 106.83, 107.77, 111.65 (d, $J = 23$ Hz), 120.24, 137.68, 145.50, 148.96, 153.33 (d, $J = 248$ Hz), 166.42, 167.12, 176.69; LC-MS (ESI) calcd for $C_{19}H_{21}FN_4NaO_7$ $[M + H]^+$: 437.15, found: 437.00

Screening of antimycobacterial activity

The used strain is *M. tuberculosis* H37Rv strain. Briefly, the inoculum was prepared from fresh LJ medium resuspended in 7H9-S medium (7H9 broth, 0.1% casitone, 0.5% glycerol, supplemented oleic acid, albumin, dextrose, and catalase), adjusted to a McFarland tube No. 1, and diluted 1:20; 100 µl was used as inoculum. Each drug stock solution was thawed and diluted in 7H9-S at four-fold the final highest concentration tested. Serial two-fold dilutions of each drug were prepared directly in a sterile 96-well microtiter plate using 100 µL 7H9-S. A growth control containing no antibiotic and a sterile control were also prepared on each plate. Sterile water was added to all perimeter wells to avoid evaporation during the incubation. The plate was covered, sealed in plastic bags and incubated at 37 °C in normal atmosphere. After 7 days incubation, 30 µL of alamar blue solution was added to each well, and the plate was re-incubated overnight. A change in color from blue (oxidized state) to pink (reduced) indicated the growth of bacteria, and the MIC was defined as the lowest concentration of drug that prevented this change in color.

Cleaved complex assay

Protein purification

M. tuberculosis GyrA and GyrB proteins were purified separately, as described previously (Blower et al. 2016). Briefly, proteins were expressed from a pET28b derivative expression plasmid, producing a TEV-cleavable hexahistadine tag at the amino-terminus. Proteins were expressed in BL21 [DE3] *E. coli* cells containing the Rosetta 2 pLysS plasmid. Cells were grown to mid-log phase at 30 °C and induced with 1 mM IPTG for 3 h. Cells were then harvested by centrifugation and resuspended in A800 buffer [30 mM Tris-HCl, pH 7.8; 800 mM NaCl; 10 mM imidazole, pH 8.0; 10% glycerol; 0.5 mM TCEP; 1 µg/mL leupeptin; 1 µg/mL pepstatin; 1 mM PMSF]. Cells were lysed by sonication and lysate was clarified by centrifugation. The soluble fraction was applied to 5 mL HisTrap HP columns and washed with 25 column volumes of A800. Captured, His_6-tagged GyrA or GyrB was eluted from the resin with B800 [30 mM Tris-HCl, pH 7.8; 800 mM NaCl; 500 mM imidazole, pH 8.0; 10% glycerol; 0.5 mM TCEP; 1 µg/mL leupeptin; 1 µg/mL pepstatin; 1 mM PMSF]. Proteins were dialyzed separately against C500 buffer [30 mM Tris-HCl, pH 7.8; 500 mM NaCl; 10 mM imidazole; 10% glycerol; 0.25 mM TCEP] in the presence of His6-tagged TEV protease; uncleaved His6-tagged tagged protein and TEV protease were removed by a second passage over a 5 mL HisTrap HP column. Cleaved proteins were concentrated and further purified by gel filtration over a sephacryl S-300HR column pre-equilibrated in A500 buffer [50 mM Tris pH 7.8; 500 mM KCl; 10% glycerol; 0.5 mM TCEP]. Fractions containing purified protein, as assessed by SDS-PAGE, were collected and concentrated. For storage, concentrated protein was mixed 1:1 with storage buffer [50 mM Tris 7.8; 500 mM KCl; 50% glycerol; 0.5 mM TCEP], then flash frozen as aliquots in liquid nitrogen and stored at −80 °C.

Cleavage assays

Fluoroquinolone compounds were resuspended in DMSO and stored at −80 °C as 2.5–10 mM stocks. Purified *M. tuberculosis* GyrA and GyrB were combined 1:1 to form the gyrase heterotetramer at a concentration of 40 µM; for assays, the holoenzyme was serially diluted in two-fold steps to a final working concentration of 1.25 µM using gyrase dilution buffer [50 mM Tris pH 7.8; 150 mM monopotassium glutamate; 5 mM MgOAc; 10% glycerol]. Cleavage assays were prepared by mixing the following on ice: 4 µL 10X supercoiled plasmid DNA (125 nM); 4 µL 10× *M. tuberculosis* gyrase heterotetramer (1.25 µM); 10 µL 4× reaction buffer [120 mM Tris pH 7.8; 38 mM MgOAc; 340 mM monopotassium glutamate; 36% glycerol; 0.4 mg/mL BSA; 4 mM TCEP]; 20 µL distilled water; 2 µL 20X fluoroquinolone compound dilutions. The final reaction conditions are as follows: 12.5 nM supercoiled DNA; 125 nM *M. tuberculosis* gyrase heterotetramer; 35 mM Tris pH 7.8; 100 mM monopotassium glutamate; 10 mM MgOAc; 10% glycerol; 100 µg/mL BSA; 1 mM TCEP; 0–500 µM fluoroquinolone compound. Cleavage reactions were conducted by incubating reactions at 37 °C in the absence of ATP for 30 min. Reactions were stopped by the addition of 2 µL 12% SDS, followed immediately by the addition of 2 µL 500 mM EDTA.

Stopped reactions were then mixed with 4 µL proteinase K (3 mg/mL) and digested at 37 °C for 25 min. Stopped and digested reaction products were then mixed with 10 µL DNA loading dye, and products were resolved by running 20 µL of the reaction-dye mix on 1.5% TAE agarose gels containing either with or without 1 µg/mL ethidium bromide (EtBr). Gels were run at 35 V for 16.5 h to resolve products and post-stained by soaking for 1 h in 1 µg/mL ethidium bromide followed by 2 h destaining in water. Gels were imaged by UV transillumination using a Gel Doc EZ gel imaging system (Bio-rad).

Acknowledgements We thank Dr. Safwat Rabea (Faculty of Pharmaceutical Sciences, The University of British Columbia, Canada), for measuring the high-resolution mass spectra for the synthesized compounds. The biochemical analysis of gyrase and the synthesized inhibitors was supported by the NCI (R01-CA077373, to J.M.B.).

Compliance with ethical standards

Conflict of interest The authors declare that they have no conflict of interest.

References

Abdel-Aziz M, Park S, Abuo-Rahma G, Sayed M, Kwon Y (2013) Novel *N*-4-piperazinyl-ciprofloxacin-chalcone hybrids: synthesis, physicochemical properties, anticancer and topoisomerase I and II inhibitory activity. Eur J Med Chem 69:427–438

Abou Rahma GE-D, Abbas S, Shoman M, Samir I, Abd El-Baky R (2018) New *N*-4 piperazinyl derivatives of norfloxacin: design, synthesis, and correlation of calculated physicochemical parameters with antibacterial activity. Turk J Chem 42:1072–1085

Abuo-Rahma G, Sarhan H, Gad G (2009) Design, synthesis, antibacterial activity and physicochemical parameters of novel N-4-piperazinyl derivatives of norfloxacin. Bioorg Med Chem 17:3879–3886

Ahmed FF, Abd El-Hafeez AA, Abbas SA, Abdelhamid D, Mohamed Abdel-Aziz (2018) New 1,2,4-triazole-Chalcone hybrids induce Caspase-3 dependent apoptosis in A549 human lung adenocarcinoma cells. Eur J Med Chem 151:705–722

AKoch A, Cox H, Mizrahi V (2018) Drug-resistant tuberculosis: challenges and opportunities for diagnosis and treatment. Curr Opin Pharmacol 42:7–15

Aldred K, Kerns R, Osheroff N (2014) Mechanism of quinolone action and resistance. Biochemistry 53:1565–1574

Aubry A, Pan X-Su, Fisher LM, Jarlier V, Cambau E (2004) *Mycobacterium tuberculosis* DNA gyrase: interaction with quinolones and correlation with antimycobacterial drug activity. Antimicrob Agents Chemother 48:1281–1288

Aziz H, Moustafa G, Abbas S, Derayea S, Abuorahma G (2017) New norfloxacin/nitric oxide donor hybrids: Synthesis and nitric oxide release measurement using a modified Griess colorimetric method. Eur J Chem 8:119–124

Barrett J, Bernstein J, Krause H, Hilliard J, Ohemeng K (1993) Testing potential gyrase inhibitors of bacterial DNA gyrase: a comparison of the supercoiling inhibition assay and and "cleavable complex" assay. Anal Biochem 214:313–317

Bi Y, Yang X, Zhang T, Liu Z, Zhang X, Lu J, Lewis P (2015) Design, synthesis, nitric oxide release and antibacterial evaluation of novel nitrated ocotillol-type derivatives. Eur J Med Chem 101:71–80

Blower TR, Williamson BH, Kerns RJ, Berger JM (2016) Crystal structure and stability of gyrase–fluoroquinolone cleaved complexes from *Mycobacterium tuberculosis*. Proc Natl Acad Sci USA 113:1706–1713

Böhmer A, Gambaryan S, Tsikas D (2015) Human blood platelets lack nitric oxide synthase activity. Platelets 26:583–588

Bryskier A, Lowther J (2002) Fluoroquinolones and tuberculosis. Expert Opin Investig Drugs 11:233–258

Champoux J (2001) DNA topoisomerases: structure, function, and mechanism. Annu Rev Biochem 70:369–413

Chugunova E, Akylbekov N, Bulatova A, Gavrilov N, Voloshina A, Kulik N, Zobov V, Dobrynin A, Syakaev V, Burilov A (2016) Synthesis and biological evaluation of novel structural hybrids of benzofuroxan derivatives and fluoroquinolones. Eur J Med Chem 116:165–172

Ciccone R, Mariani F, Cavone A, Persichini T, Venturini G, Ongini E, Colizzi V, Colasanti M (2003) Inhibitory effect of NO-releasing ciprofloxacin (NCX 976) on *Mycobacterium tuberculosis* survival. Antimicrob Agents Chemother 47:2299–2302

Clementi E, Brown G, Foxwell N, Moncada S (1999) On the mechanism by which vascular endothelial cells regulate their oxygen consumption. Proc Natl Acad Sci USA 96:1559–1562

Cooke J, Mont-Reynaud R, Philip S, Maxwell A (2000) Nitric oxide and vascular disease. Nitric Oxide: Biology and Pathology. In: Ignarro LJ (ed) Academic Press, New York, p 759–783

D'Autréaux B, Touati D, Bersch B, Latour J, Michaud S (2002) Direct inhibition by nitric oxide of the transcriptional ferric uptake regulation protein via nitrosylation of the iron. Proc Natl Acad Sci USA 99:16619–16624

Fang F (2004) Antimicrobial reactive oxygen and nitrogen species: concepts and controversies. Nature Rev Microbiol 2:820–832

Gardner P, Costantino G, Szabó C, Salzman A (1997) Nitric oxide sensitivity of the aconitases. J Biol Chem 272:25071–25076

Gillespie S, Crook A, McHugh T, Mendel C, Meredith S, Murray S, Pappas F, Philips P, Andrew J (2014) Four-month moxifloxacin-based regimens for drug-sensitive tuberculosis. New Eng J Med 371:1577–1587

Guerrini V, De Rosa M, Pasquini S, Mugnaini C, Brizzi A, Cuppone A, Pozzi G, Corelli F (2013) New fluoroquinolones active against fluoroquinolones-resistant *Mycobacterium tuberculosis* strains. Tuberculosis 93:405–411

Hooper D (2001) Emerging mechanisms of fluoroquinolone resistance. Emerg Infect Dis 7:337–341

Khaund K, Sudhakar C, Charlet JaSmiNe Vaz CJ (2018) Infection control prevention practices on pulmonary TB transmission among health care personnel of selected hospital in India. JCDR 12(11):10–15

Kłosińska-Szmurło E, Pluciński FA, Grudzień M, Betlejewska-Kielak K, Biernacka J, Mazurek AP (2014) Experimental and theoretical studies on the molecular properties of ciprofloxacin, norfloxacin, pefloxacin, sparfloxacin, and gatifloxacin in determining bioavailability. J Biol Phys 40(4):335–345

Long R, Light B, Talbot J (1999) Mycobacteriocidal action of exogenous nitric oxide. Antimicrob Agents Chemother 43:403–405

Merle C, Fielding K, Sow O, Gninafon M, Lo M, Mthiyane T, Odhiambo J, Amukoye E, Bah B, Kassa F, Ndiaye A (2014) A four-month gatifloxacin-containing regimen for treating tuberculosis. New Eng J Med 371:1588–1598

Miltgen J, Morillon M, Koeck J, Varnerot A, Briant J, Nguyen G, Verrot D, Bonnet D, Vincent V (2002) Two cases of pulmonary tuberculosis caused by *Mycobacterium tuberculosis* subsp. canetti. Emerg Infect Dis 8:1350–1352

Mohammeda HH, Abd El-Hafeez AA, Abbas SH, E-S M Abdelhafez El-SM, Abuo-Rahma GE-D (2016) New antiproliferative 7-(4-(N-substituted carbamoylmethyl)piperazin-1-yl) derivatives of ciprofloxacin induce cell cycle arrest at G2/M phase. Bioorg Med Chem 24:4636–4646

Mustaev A, Malik M, Zhao X, Kurepina N, Luan G, Oppegard LM, Hiasa H, Marks KR, Kerns RJ, Berger JM, Drlica K (2014) Fluoroquinolone-gyrase-DNA complexes two modes of drug binding. J Biol Chem 289:12300–12312

Pitsikas N (2015) The role of nitric oxide in the object recognition memory. Behav Brain Res 285:200–207

Porasuphatana S, Tsai P, Rosen G (2003) The generation of free radicals by nitric oxide synthase. Comp Biochem Physiol Part C 134:281–289

Shi H, Efron D, Most D, Tantry U, Barbul A (2000) Supplemental dietary arginine enhances wound healing in normal but not inducible nitric oxide synthase knockout mice. Surgery 128:374–378

Sotgiu G, Migliori G (2015) Facing multi-drug resistant tuberculosis. Pulm Pharmacol Ther 32:144–148

Sriram D, Yogeeswari P, Basha J, Radha D, Nagaraja V (2005) Synthesis and antimycobacterial evaluation of various 7-substituted ciprofloxacin derivatives. Bioorg. Med Chem 13:5774–5778

Talath S, Gadad A (2006) Synthesis, antibacterial and antitubercular activities of some 7-[4-(5-amino-[1, 3, 4] thiadiazole-2-sulfonyl)-piperazin-1-yl] fluoroquinolonic derivatives. Eur J Med Chem 41:918–924

The methodology of the NCI anticancer screening has been described in details: (http://www.dtp.nci.nih.gov), Bethesda, USA

Timmins G, Master S, Rusnak F, Deretic V (2004) Nitric oxide generated from isoniazid activation by KatG: source of nitric oxide and activity against *Mycobacterium tuberculosis*. Antimicrob Agents Chemother 48:3006–3009

Trinity J, Groot H, Layec G, Rossman M, Ives S, Morgan D, Gmeleh B, Bledsoe A, Richardson R (2015) Passive leg movement and nitric oxide-mediated vascular function: the impact of age. Am J Physiol Heart Circ Physiol 308:672–679

Vahora H, Khan M, Alalami U, Hussain A (2016) The potential role of nitric oxide in halting cancer progression through chemoprevention. J Cancer Prev 21:1–12

Vaitilingam B, Nayyar A, Palde P, Monga V, jain R, Kaur S, Singh P (2004) Synthesis and antimycobacterial activities of ring-substituted quinolinecarboxylic acid/ester analogues. Bioorg Med Chem 12:4179–4188

Wallace J, Reuter B, Cicala C, McKnight W, Grisham M, Cirino G (1994) A diclofenac derivative without ulcerogenic properties. Eur J Pharmacol 257:249–255

World Health Organization (2017) Global Tuberculosis Report 2017. World Health Organization, Geneva